



Fluorescence Properties of Fe^{2+} - and Co^{2+} -doped Hosts of CdMnTe Compositions as Potential Mid-Infrared Laser Materials

by Tigran Sanamyan, Sudhir Trivedi, and Mark Dubinskii

ARL-TR-5770

September 2011

NOTICES

Disclaimers

The findings in this report are not to be construed as an official Department of the Army position unless so designated by other authorized documents.

Citation of manufacturer's or trade names does not constitute an official endorsement or approval of the use thereof.

Destroy this report when it is no longer needed. Do not return it to the originator.

Army Research Laboratory

Adelphi, MD 20783-1197

ARL-TR-5770**September 2011**

Fluorescence Properties of Fe^{2+} - and Co^{2+} -doped Hosts of CdMnTe Compositions as Potential Mid-Infrared Laser Materials

Tigran Sanamyan and Mark Dubinskii
Sensors and Electron Devices Directorate, ARL

Sudhir Trivedi
Brimrose Corporation, Sparks, MD

REPORT DOCUMENTATION PAGE				Form Approved OMB No. 0704-0188	
<p>Public reporting burden for this collection of information is estimated to average 1 hour per response, including the time for reviewing instructions, searching existing data sources, gathering and maintaining the data needed, and completing and reviewing the collection information. Send comments regarding this burden estimate or any other aspect of this collection of information, including suggestions for reducing the burden, to Department of Defense, Washington Headquarters Services, Directorate for Information Operations and Reports (0704-0188), 1215 Jefferson Davis Highway, Suite 1204, Arlington, VA 22202-4302. Respondents should be aware that notwithstanding any other provision of law, no person shall be subject to any penalty for failing to comply with a collection of information if it does not display a currently valid OMB control number.</p> <p>PLEASE DO NOT RETURN YOUR FORM TO THE ABOVE ADDRESS.</p>					
1. REPORT DATE (DD-MM-YYYY) September 2011		2. REPORT TYPE Final		3. DATES COVERED (From - To)	
4. TITLE AND SUBTITLE Fluorescence Properties of Fe ²⁺ - and Co ²⁺ -doped Hosts of CdMnTeCompositions as Potential Mid-Infrared Laser Materials				5a. CONTRACT NUMBER	
				5b. GRANT NUMBER	
				5c. PROGRAM ELEMENT NUMBER	
6. AUTHOR(S) Tigran Sanamyan, Sudhir Trivedi, and Mark Dubinskii				5d. PROJECT NUMBER	
				5e. TASK NUMBER	
				5f. WORK UNIT NUMBER	
7. PERFORMING ORGANIZATION NAME(S) AND ADDRESS(ES) U.S. Army Research Laboratory ATTN: RDRL-SEE-M 2800 Powder Mill Road Adelphi, MD 20783-1197				8. PERFORMING ORGANIZATION REPORT NUMBER ARL-TR-5770	
9. SPONSORING/MONITORING AGENCY NAME(S) AND ADDRESS(ES)				10. SPONSOR/MONITOR'S ACRONYM(S)	
				11. SPONSOR/MONITOR'S REPORT NUMBER(S)	
12. DISTRIBUTION/AVAILABILITY STATEMENT Approved for public release; distribution unlimited.					
13. SUPPLEMENTARY NOTES					
14. ABSTRACT Solid-state laser sources emitting in a mid-infrared (IR) spectral range are of significant practical interest due to the great variety of potential applications in the biomedical industry, remote sensing, pollution monitoring, molecular spectroscopy, residual gas tracing, and IR countermeasures. The need for mid-IR wavelengths directly obtainable from a diode-pumped solid-state gain medium stimulates searches for new laser materials with wide tunability. We report the results of spectroscopic investigation of Fe ²⁺ - and Co ²⁺ -doped low-phonon single crystals of the cadmium telluride (CdTe) family. It is shown that compositional changes of the host material significantly affect the radiative lifetime of the initial laser level, the bandwidth of the emission and absorption spectra, and their overall positioning, which will translate into potential mid-IR laser threshold and tunability. Single crystal composition also affects the Co ²⁺ and Fe ²⁺ dopant lifetimes and temperature dependencies. Crystal growth effort is underway in order to improve the quality of the samples toward satisfying laser-grade loss figure requirements.					
15. SUBJECT TERMS Transitional metal, cadmium telluride, mid-IR, tunable, laser					
16. SECURITY CLASSIFICATION OF:			17. LIMITATION OF ABSTRACT UU	18. NUMBER OF PAGES 22	19a. NAME OF RESPONSIBLE PERSON Tigran Sanamyan
a. REPORT Unclassified	b. ABSTRACT Unclassified	c. THIS PAGE Unclassified			19b. TELEPHONE NUMBER (Include area code) (301) 394-2044

Contents

List of Figures	iv
List of Tables	iv
1. Introduction	1
2. Experimental Setup	2
3. Results and Discussions	4
4. Conclusions	10
5. References	11
List of Symbols, Abbreviations, and Acronyms	13
Distribution List	15

List of Figures

Figure 1. Typical as grown samples of undoped CMT.....	3
Figure 2. Transmission spectrum of the undoped CdTe grown at Brimrose Corporation (Nicolet 8700 FTIR Spectrometer).	5
Figure 3. Fluorescence spectra corresponding to the $^5T_2 \rightarrow ^5E$ transition of the Fe^{2+} doped Cd(0.85%)Mn(0.15%)Te and Cd(0.55%)Mn(0.45%)Te samples.	5
Figure 4. Fluorescence lifetime ($^5T_2 \rightarrow ^5E$ transition) vs. temperature for the Fe^{2+} doped Cd(0.85%)Mn(0.15%)Te and Cd(0.55%)Mn(0.45%)Te samples.	6
Figure 5. Fluorescence spectrum of Fe^{2+} -doped Cd(0.65%)Mg(0.15%)Mn(0.2%)Te corresponding to $^5T_2 \rightarrow ^5E$ transition. As a reference, the fluorescence spectrum of Fe^{2+} -doped Cd(0.85%)Mn(0.15%)Te is shown as well.	7
Figure 6. Absorption spectra of Fe^{2+} -doped Cd(0.65%)Mg(0.15%)Mn(0.2%)Te at RT and LNT corresponding to $^5E \rightarrow ^5T_2$ transition.	7
Figure 7. Emission cross-section of Fe^{2+} doped Cd(0.65%)Mg(0.15%)Mn(0.2%)Te corresponding to the $^5T_2 \rightarrow ^5E$ transition of Fe^{2+} at LNT converted from the fluorescence spectra shown in figure 5.	8
Figure 8. LNT fluorescence spectrum of Co^{2+} doped Cd(0.95%)CoMg(0.05%)Te corresponding to $^4T_2 \rightarrow ^4A_2$ transition.	9
Figure 9. Co^{2+} 4T_2 level fluorescence lifetime versus temperature for Co^{2+} doped Cd(0.95%)CoMg(0.05%)Te.	9

List of Tables

Table 1. Maximum phonon frequency (cm^{-1}).....	2
------------------------------------------------------	---

1. Introduction

Solid-state mid-infrared (IR) laser sources emitting in a 3–7 μm spectral range are of significant practical interest due to great variety of potential applications in the biomedical industry, remote sensing, pollution monitoring, etc. They can be used in molecular spectroscopy, residual gas tracing, IR countermeasures (IRCM), improvised explosive device (IED) detection, eye-safe sensors for lidar, and medical applications. The detailed review of recent advances in mid-IR laser materials operating in the 3–5 μm wavelength range can be found in references 1 and 2. Today this spectral range is covered by lasers and laser systems based on nonlinear frequency conversion techniques, for example, optical parametric oscillators or amplifiers, most often using high power neodymium laser as a fundamental frequency pump source. These optical parametric oscillator (OPO) sources have obvious disadvantages—complexity, inefficiency, and high cost—compared to direct diode-pumped solid-state lasers. The need for mid-IR wavelengths directly obtainable from a diode-pumped solid-state gain medium stimulates searches for new laser materials with wide tunability. In references 3 and 4, laser action of divalent chromium ion (Cr^{2+}): zinc selenide (ZnSe) in the 2.1–2.9 μm spectral range has been demonstrated, and the Cr^{2+} :ZnSe laser is further developed in reference 5. Laser action around 3.55 μm from a divalent iron ion (Fe^{2+}) in low-phonon semiconductors has been demonstrated (6). Later, a widely tunable laser action between 4.0–4.5 μm was demonstrated in Fe^{2+} -doped ZnSe operating below 180 K (7). Unfortunately, so far, only a limited number of materials that lase in the mid-IR region have been found to have a sufficiently high efficiency at room temperature (RT), and only very few of them, like Cr^{2+} :ZnSe, have been introduced to the solid-state laser market. The choice of Cr^{2+} :ZnSe was particularly motivated by the unique advantageous combination of this material's optical, laser, spectroscopic, and thermo-mechanical properties.

Transitional metal (TM) ion doped oxides, fluorides, and chalcogenides historically were the first tunable solid-state laser sources with a wide tunability range in the near- and mid-IR spectral ranges since the advent of the laser in the early 1960s (see reference 8 and references therein). This tunability is possible due to the intrinsically broad spectral emission nature of 3d-3d transitions in TM. There was considerable work done on Cr- and Fe-doped binary ZnSe, zinc sulfide (ZnS), cadmium selenide (CdSe), cadmium sulfide (CdS), zinc telluride (ZnTe), or ternary cadmium manganese telluride (CdMnTe or CMT), cadmium zinc telluride (CdZnTe), and zinc sulfur selenide (ZnSSe) chalcogenide crystals (1). Among the TM ions, Cr^{2+} was extensively explored in ZnSe and ZnS and up to tens of watts of continuous wave (CW) power with an efficiency over 40% and a wide tunability range has been demonstrated in Cr^{2+} :ZnSe (9, 10).

The Fe^{2+} ion has a similar to Cr^{2+} electronic structure with a ^5D ground state. In most materials, the maximum of broadband absorption for Fe^{2+} is located around $3\text{ }\mu\text{m}$ and the broad emission bandwidth reaches up to $1.5\text{ }\mu\text{m}$, corresponding to the transition $^5\text{T}_2 \rightarrow ^2\text{E}$. In all known hosts, the fluorescence from the upper $^5\text{T}_2$ state is quenched at RT. The RT quantum efficiency is less than 1% and the lifetime ends up being as short as $1\text{ }\mu\text{s}$.

Recently, a relatively new CdTe-based II–VI semiconductor family of materials has been introduced as a promising host for mid-IR lasers (11–13). These hosts offer some advantages compared to the well-known ZnSe. These new materials are primarily Cr^{2+} -doped cadmium and CMT, and their properties have been extensively studied (14, 15). Similar to ZnSe in cadmium telluride (CdTe), the TM ions occupy tetrahedral sites. In the case of the Fe^{2+} ion, this results in relatively small energy splitting of the ground ^5D state due to the smaller (compared to octahedral or cubic symmetries) crystal field parameter Dq . In addition, Fe^{2+} has a smaller effective ionic radius than Cr^{2+} . Because of the two reasons mentioned earlier, the absorption and emission spectra of $\text{Fe}^{2+}:\text{CdTe}$ are shifted towards longer wavelengths and exhibit very broad emission spectra located around $3.5\text{--}5.2\text{ }\mu\text{m}$. Furthermore, the presence of the heavier chalcogen ion (Te) decreases the phonon cut-off frequency in CdTe. Table 1 shows the maximum phonon frequency for some II-VI host materials. As shown in table 1, CdTe has the lowest phonon cut-off frequency compared to all presented host materials. The low phonon frequency adds two favorable qualities to CdTe as a host for mid-IR lasers. It mitigates the nonradiative relaxation process from the upper (fluorescent) electronic states and extends the IR transparency at the long-wavelength end of the spectrum beyond $20\text{ }\mu\text{m}$. Another attractive feature of CdTe is that this material combines useful properties of dielectric and semiconductor materials. This opens an alternative of direct electrical pumping by running the electrical current through the medium as opposed to optical pumping. The first RT laser operation of iron-doped ZnSe around the $3.9\text{--}5.0\text{ }\mu\text{m}$ spectral range was reported in references 16 and 17. The search for new laser materials capable of direct lasing over the $4\text{--}7\text{ }\mu\text{m}$ spectral range remains one of the important research directions aimed at development of new mid- IR solid-state materials.

Table 1. Maximum phonon frequency (cm^{-1}).

Host Material	CdTe	ZnSe	ZnS	YLF	YAG
Phonon Cut-off Frequency (cm^{-1})	210	250	350	560	850

Note: YLF = yttrium lithium fluoride and YAG = yttrium aluminum garnet.

2. Experimental Setup

The ternary compound semiconductor $\text{Cd}(1-x)\text{Mn}(x)\text{Te}$ crystallizes in the cubic zinc-blende structure, up to $x=0.77$. Different techniques have been developed for fabrication of II-VI bulk material. Among those are melt growth, physical vapor transport (PVD), and chemical vapor

transport (CVD). The melt growth technique is the preferred method of growing CMT crystals. The addition of magnesium telluride (MnTe) to CdTe suppresses the melting point CdTe and the CdTe-MnTe pseudo-binary phase diagram does not have a separation between solidus and liquidus lines up to about 45% of MnTe. Thus, the problem of segregation in Cd(1-x)Mn(x)Te, up to x=0.45 does not exist, and single crystals of this ternary compound up to x=0.45 can be grown with excellent compositional homogeneity. A variety of single-crystalline samples of Fe²⁺ or divalent cobalt ion (Co²⁺)-doped CMT crystals were produced by Brimrose Corporation using a modified vertical Bridgman technique (18). The starting high purity ingredients Cd, Mn, and Te along with the dopants (Fe and Co) are placed in a pre-cleaned and baked graphitized quartz ampoule and vacuum (10⁻⁶ Torr) sealed. The ampoule is then placed in a three-zone, vertical Bridgman furnace. The furnace is then ramped up to 1100 °C in a predetermined sequence to react and melt these ingredients safely. The melt is allowed to mix for 24 h and translated down at a rate of 1.5 mm/h through a temperature gradient of 25 °C/cm. Upon completion of the crystal growth, the furnace is slowly cooled down to RT in about 24 h. Figure 1 shows typical as-grown samples of CMT. The dopant concentrations varied between 10¹⁹ and 5x10¹⁹ cm⁻³. For our absorption and fluorescence studies, the grown samples were cut and polished into 3–5 mm thick pieces.



Figure 1. Typical as-grown samples of undoped CMT.

The spectroscopic-grade CMT samples were mounted in a low temperature standard Oxford Instruments cryostat, which employed liquid nitrogen as a refrigerant. The cryostat was equipped with two calcium fluoride uncoated windows fully transparent in mid-IR. Various diode lasers with wavelengths in the range of 808–3200 nm, and occasionally, a tunable titanium (Ti):sapphire laser (750–1000 nm), were used for fluorescence excitation. The RT and liquid nitrogen temperature (LNT) unpolarized absorption spectra were taken using either a Cary 5000i spectrophotometer or a Nicolet 8700 FT-IR spectrometer. The luminescence spectra were studied using a 0.5-m Acton Research 2500i monochromator coupled with liquid-nitrogen-cooled

indium antimonide (InSb) or MCT detectors. The spectral resolution in all spectral measurements was better than 10 nm. The detected signal was processed by a Stanford research SR-250 gated integrator and boxcar averager or an SR 850 Lock-In amplifier, and acquired through the NI-DAQmx acquisition interface in the LabVIEW environment.

The lifetime measurements were carried out under sample excitation by nanosecond pulses from tunable Ti:Sapphire laser in the wavelength range of 800–900 nm. The fluorescence decay signal was detected by a high-speed Judson J10D-M204-R02M-60 detector at the peak of fluorescence band and processed (averaged) using a digitizing oscilloscope, Tektronix TDS 2022B.

3. Results and Discussions

Table 1 summarizes the maximum phonon cut-off frequencies (determined from Raman scattering spectra) for a variety of well-known crystalline solid-state laser hosts compiled for comparison. As can be seen from table 1, CdTe-based chalcogenide has the lowest phonon cut-off frequency, which maximizes the probability of nearly purely radiative decay of mid-IR fluorescence in this crystal.

Furthermore, cut-off frequency affects the long-wavelength transparency of the host material. Figure 2 shows the transmission spectrum of undoped CdTe, which clearly indicates that the host transparency is well beyond 20 μm . Figure 3 presents the fluorescence spectra of the Fe^{2+} -doped $\text{Cd}(0.55\%)\text{Mn}(0.45\%)\text{Te}$ and $\text{Cd}(0.85\%)\text{Mn}(0.15\%)\text{Te}$ samples. Despite the significant compositional difference, namely, the large change in Mn concentration in the two samples, no substantial change in the emission spectra was observed. Despite the similarity of emission spectra, the lifetime of initial $^5\text{T}_2$ state of Fe^{2+} fluorescence in these hosts differs significantly. Thus, as shown in figure 4, the lifetime of the $\text{Fe}^{2+} ^5\text{T}_2$ level in $\text{Cd}(0.85\%)\text{Mn}(0.15\%)\text{Te}$ appears to be approximately 30% longer than that of the $\text{Fe}^{2+} ^5\text{T}_2$ level in $\text{Cd}(0.55\%)\text{Mn}(0.45\%)\text{Te}$. This indicates that lower doping Mn concentrations are more favorable in achieving higher fluorescence efficiency. The drastic lifetime reduction of the $\text{Fe}^{2+} ^5\text{T}_2$ state in both samples at temperatures above 120 K can be explained by the rapid onset of thermally activated nonradiative multiphonon decay. The measured lifetime and fluorescence quantum yield at RT for both samples were several hundreds of ns and less than 1%, respectively.

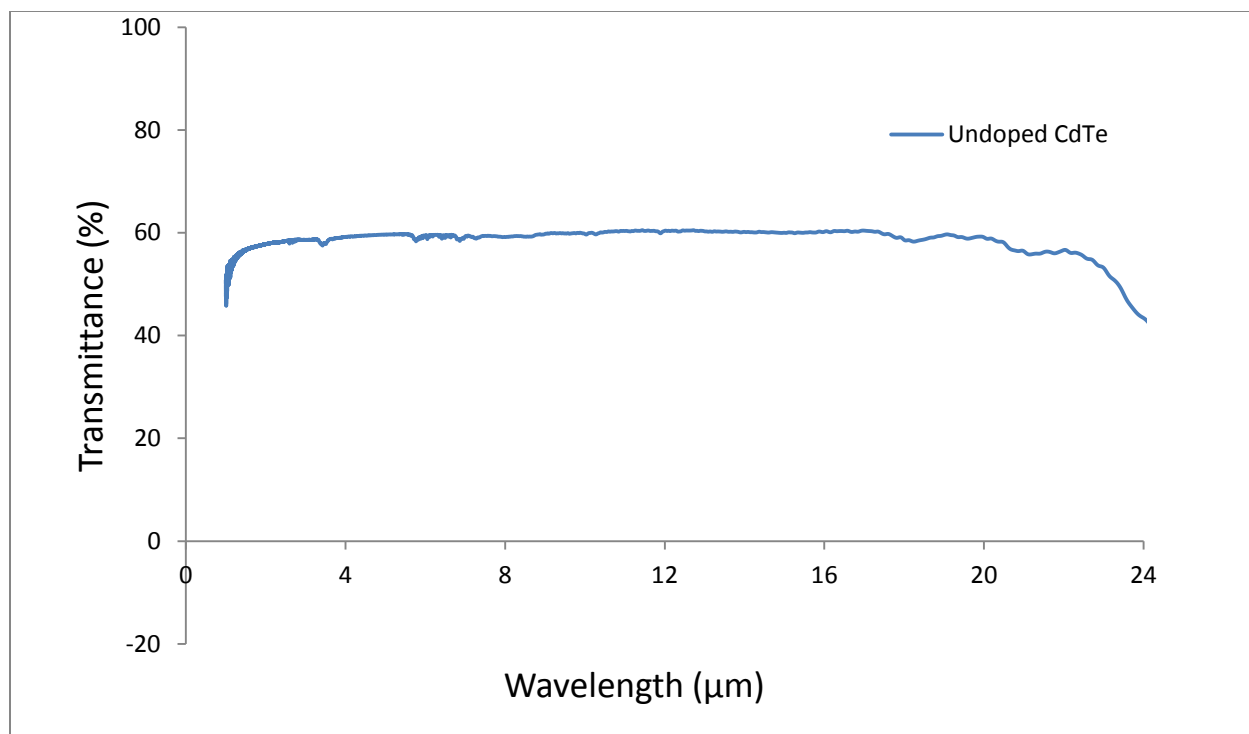


Figure 2. Transmission spectrum of the undoped CdTe grown at Brimrose Corporation (Nicolet 8700 FTIR spectrometer).

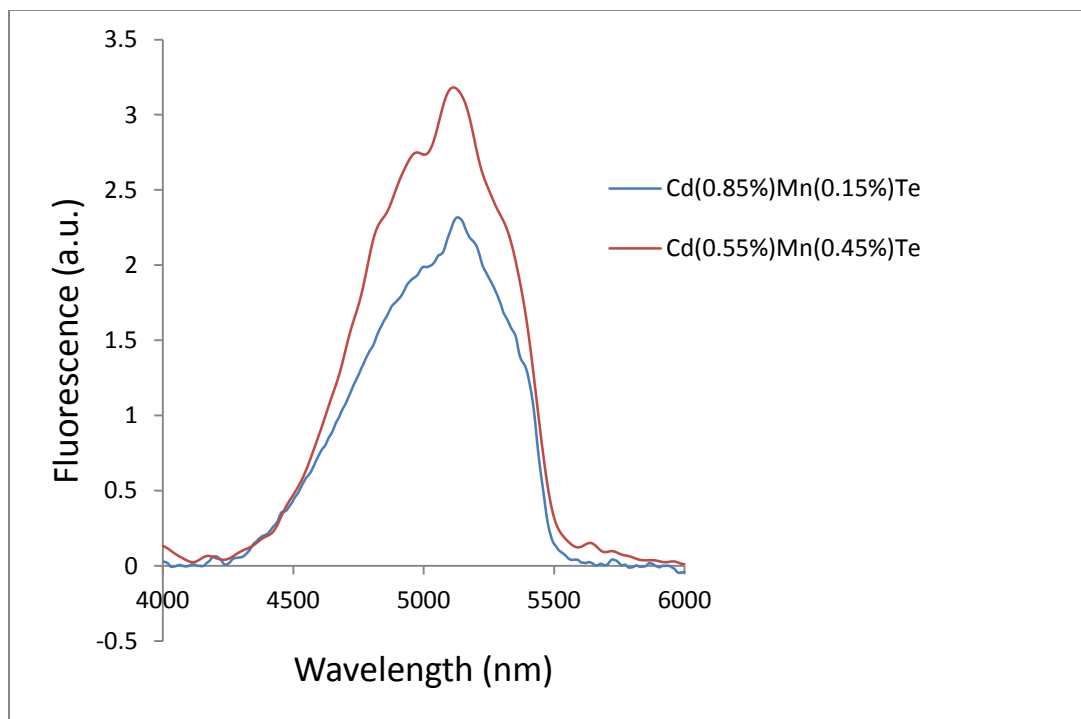


Figure 3. Fluorescence spectra corresponding to the ${}^5T_2 \rightarrow {}^5E$ transition of the Fe^{2+} -doped Cd(0.85%)Mn(0.15%)Te and Cd(0.55%)Mn(0.45%)Te samples.

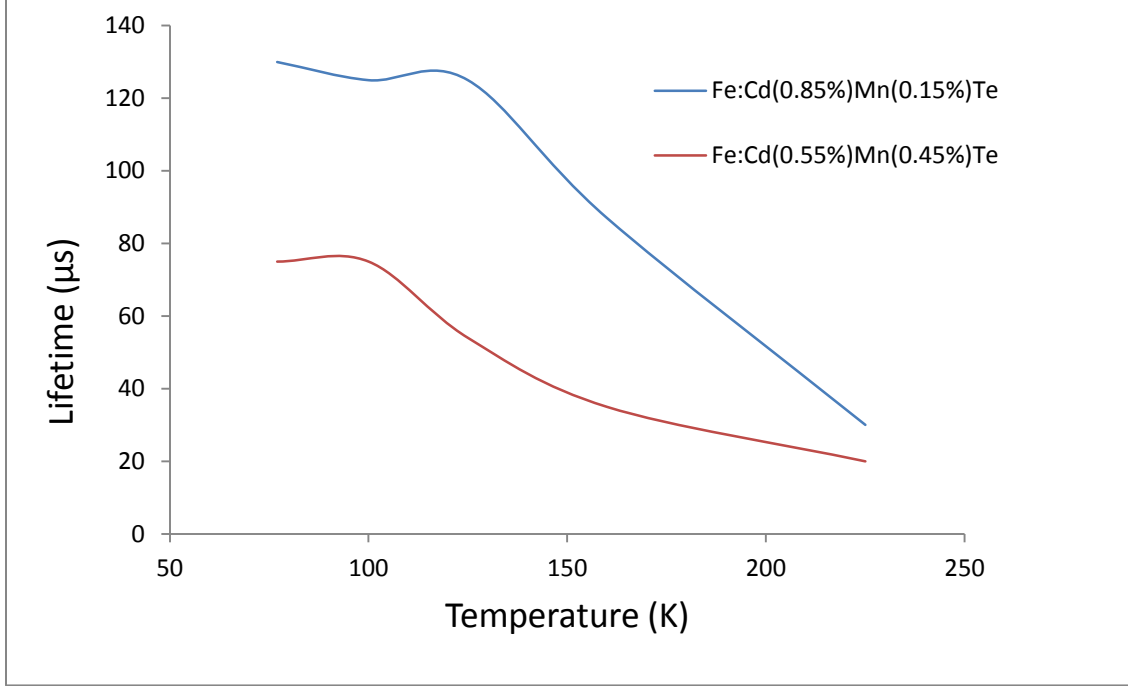


Figure 4. Fluorescence lifetime ($^5T_2 \rightarrow ^5E$ transition) vs. temperature for the Fe^{2+} -doped Cd(0.85%)Mn(0.15%)Te and Cd(0.55%)Mn(0.45%)Te samples.

The Fe^{2+} -doped CdTe samples exhibit quite different behavior when they are co-doped with magnesium (Mg) ions. Figure 5 indicates the LNT fluorescence spectrum of the Fe^{2+} -doped Cd(0.65%)Mg(0.15%)Mn(0.2%)Te sample along with the Fe^{2+} -doped Cd(0.55%)Mn(0.45%)Te sample as a reference. It can be seen that the addition of 0.15% of Mg is shifting the emission spectrum peak by approximately 400 nm towards longer wavelength. The measured fluorescence lifetime of the $Fe^{2+} \ ^5T_2$ state was about 100 μs at 77 K. The measured absorption spectra of Fe^{2+} -doped Cd(0.65%)Mg(0.15%)Mn(0.2%)Te at RT and LNT are shown in figure 6. At both temperatures, the spectra feature a wide absorption range between 3000–5000 nm with the peak around 3900 nm. As the temperature grows from 77 to 300 K, the absorption bandwidth becomes wider with a slight decrease of the peak absorption. The emission spectrum of Fe^{2+} -doped Cd(0.65%)Mg(0.15%)Mn(0.2%)Te shown in figure 5 was converted into an emission cross section via a Fuchtbauer-Landerburg (F-L) derivation (19):

$$\sigma = \frac{\lambda^4 A_{rad}}{8\pi c n^2} q(\lambda) \quad (1)$$

where σ is the emission cross section; n - refractive index (equals 2.4 for CdTe); $q(\lambda)$ is normalized emission spectrum; and A_{rad} is the probability of spontaneous transition between the 5T_2 and 5E states. In F-L calculations, we assumed that at LNT the nonradiative quenching of 5E level is negligible and the transition is purely radiative with $A_{rad}=1/\tau$, where τ is experimentally measured lifetime for $\sim 5\text{-}\mu m$ transition. Figure 7 shows calculated emission cross section for Fe^{2+} in Cd(0.65%)Mg(0.15%)Mn(0.2%)Te. As seen from figure 7, the peak value of emission cross section at $\sim 4.5 \mu m$ reaches $2.6 \times 10^{-18} \text{ cm}^2$ at LNT.

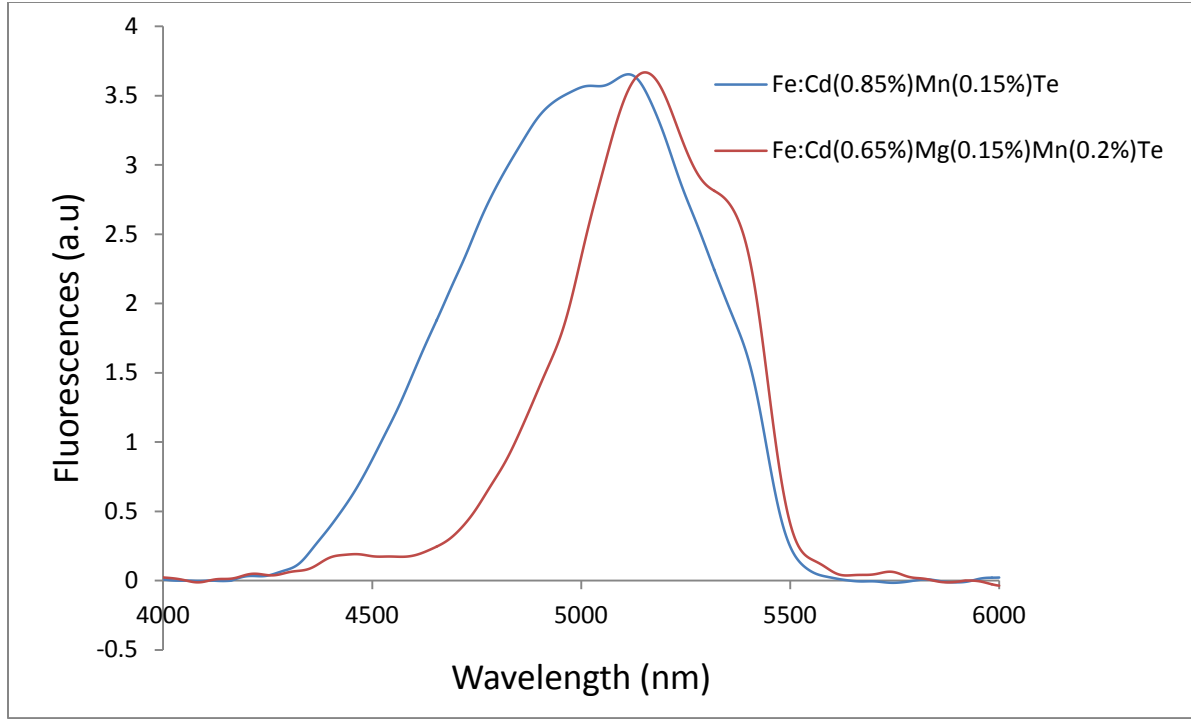


Figure 5. Fluorescence spectrum of Fe^{2+} -doped $\text{Cd}(0.65\%)\text{Mg}(0.15\%)\text{Mn}(0.2\%)\text{Te}$ corresponding to ${}^5\text{T}_2 \rightarrow {}^5\text{E}$ transition. As a reference, the fluorescence spectrum of Fe^{2+} -doped $\text{Cd}(0.85\%)\text{Mn}(0.15\%)\text{Te}$ is shown as well.

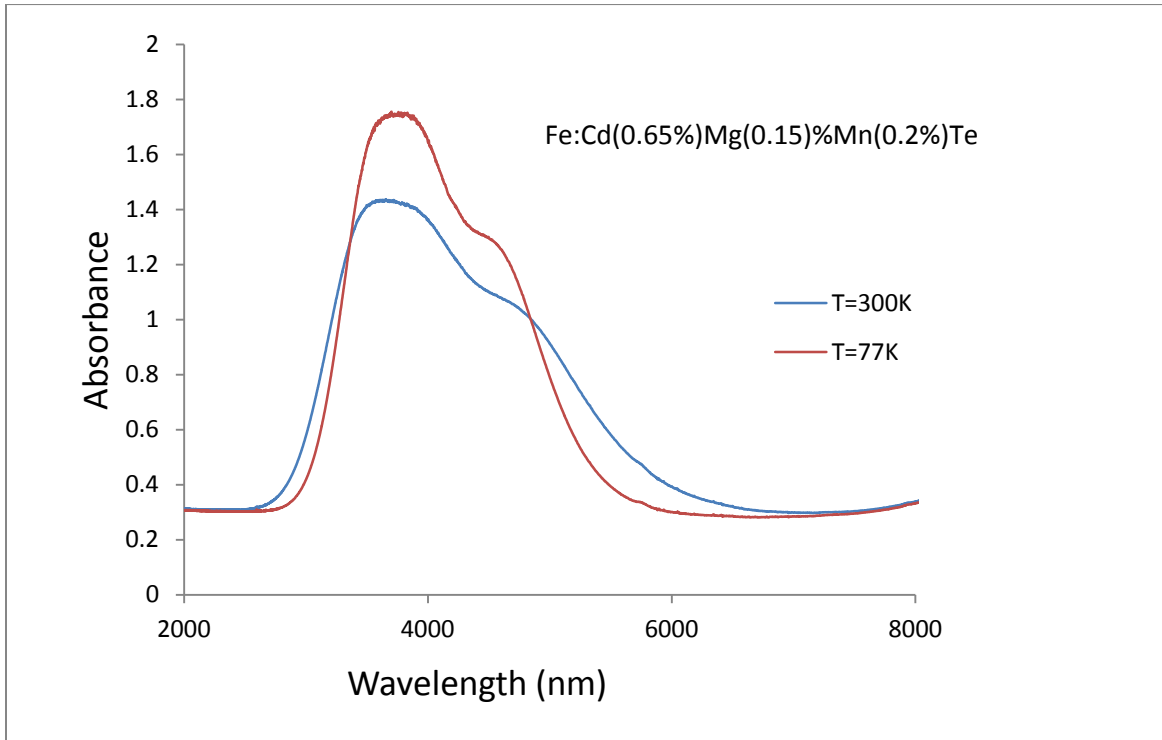


Figure 6. Absorption spectra of Fe^{2+} -doped $\text{Cd}(0.65\%)\text{Mg}(0.15\%)\text{Mn}(0.2\%)\text{Te}$ at RT and LNT corresponding to ${}^5\text{E} \rightarrow {}^5\text{T}_2$ transition.

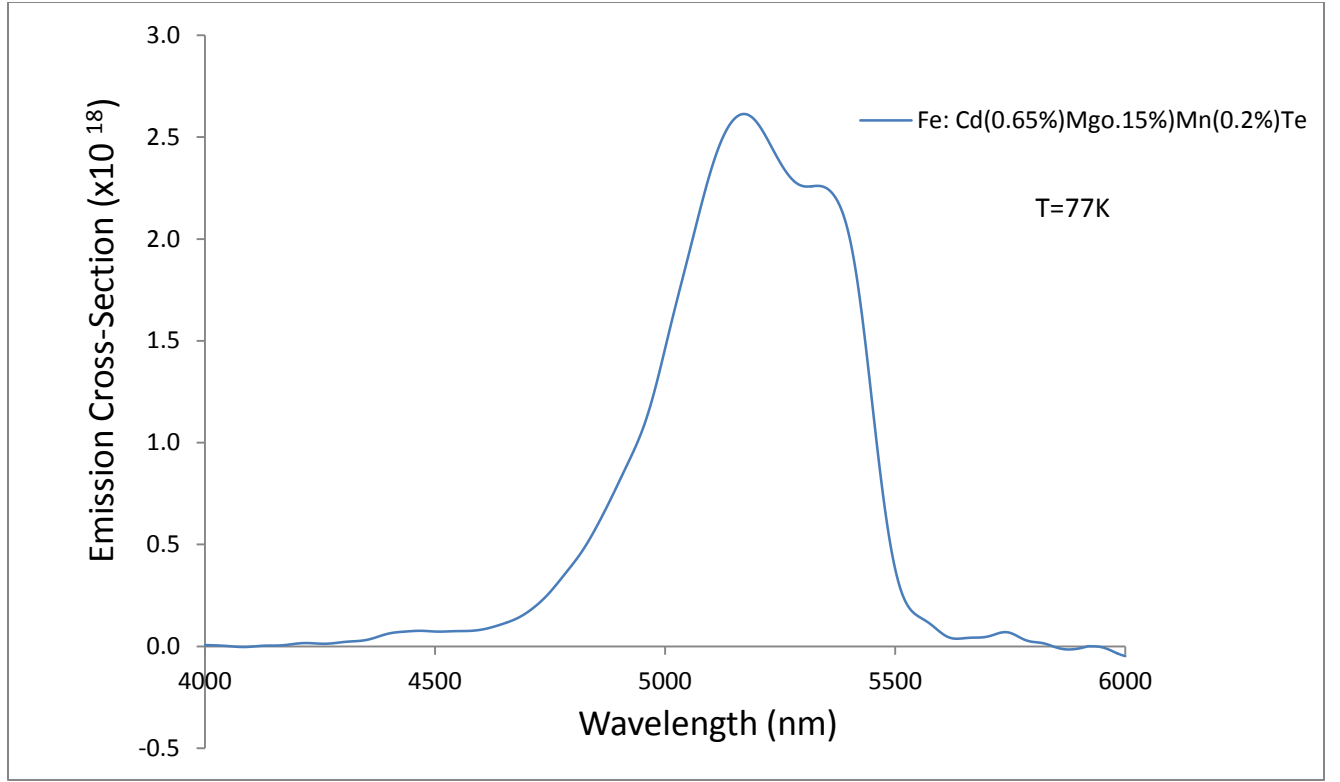


Figure 7. Emission cross-section of Fe^{2+} doped $\text{Cd}(0.65\%)\text{Mg}(0.15\%)\text{Mn}(0.2\%)\text{Te}$ corresponding to the ${}^5\text{T}_2 \rightarrow {}^5\text{E}$ transition of Fe^{2+} at LNT converted from the fluorescence spectra shown in figure 5.

A Co^{2+} ion holds an intermediate wavelength position between Cr^{2+} and Fe^{2+} , and hence, has its own niche in IRCM applications. So, we also studied the spectroscopy of Co^{2+} ions in CMT hosts. Figures 8 and 9 show fluorescence features of the upper ${}^4\text{T}_2$ level of Co^{2+} ions in $\text{Cd}(0.95\%)\text{Co}(0.05\%)\text{Te}$ corresponding to ${}^4\text{T}_2 \rightarrow {}^4\text{A}_2$ transition at cryogenic temperatures. The observed wide fluorescence spectrum and relatively long lifetime of the ${}^4\text{T}_2$ manifold are in good agreement with those observed for other Co^{2+} -doped materials (3). As shown in figure 9, the lifetime of the ${}^4\text{T}_2$ state is pretty long, exceeding 700 μs at 77 K, and does not change considerably within the temperature range of 70–110 K. This relatively long lifetime of the fluorescent level makes Co^{2+} -doped CdTe quite a promising material for diode-pumped mid-IR solid-state lasers.

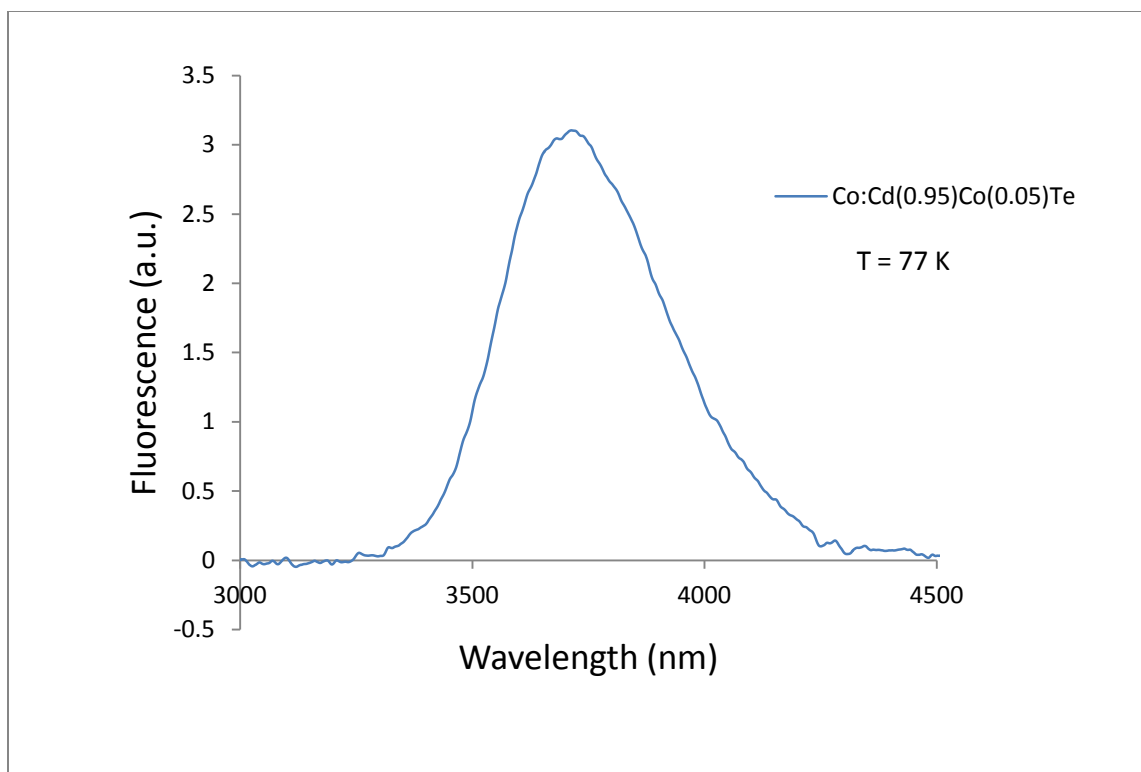


Figure 8. LNT fluorescence spectrum of Co^{2+} -doped $\text{Cd}(0.95\%)\text{CoMg}(0.05\%)\text{Te}$ corresponding to ${}^4\text{T}_2 \rightarrow {}^4\text{A}_2$ transition.

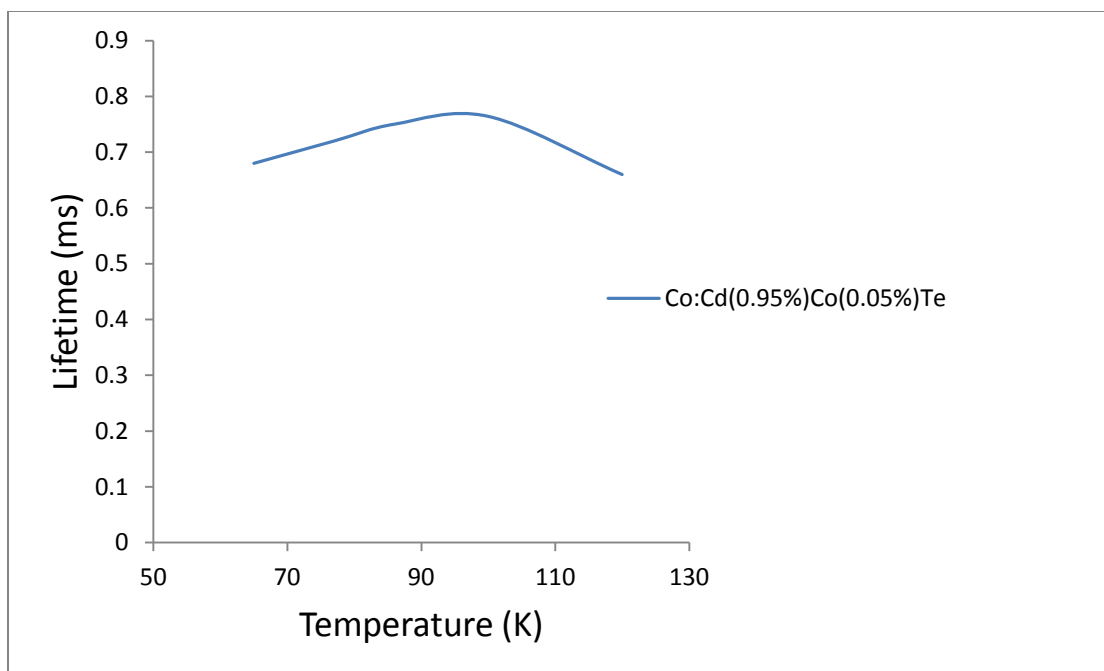


Figure 9. $\text{Co}^{2+} {}^4\text{T}_2$ level fluorescence lifetime versus temperature for Co^{2+} -doped $\text{Cd}(0.95\%)\text{CoMg}(0.05\%)\text{Te}$.

4. Conclusions

We report the results of a spectroscopic investigation of Fe^{2+} - and Co^{2+} -doped low-phonon single crystals of the CdTe family. It is shown that compositional changes of the host material significantly affect the radiative lifetime of the initial laser level, the bandwidth of the emission and absorption spectra, and their overall positioning. These will translate into a potential mid-IR laser threshold and tunability. Single crystal composition also affects the Co^{2+} and Fe^{2+} dopant lifetimes, as well as their temperature dependencies. Crystal growth effort is underway in order to improve the quality of the samples toward meeting the “laser-acceptable” loss figure requirements.

5. References

1. Mirov, S.; Fedorov, V.; Moskalev, I.; Martyshkin, D.; Kim, C. *Laser & Photon. Rev.* **2010**, 4, 21.
2. Kaminskii, A. *Laser & Photon. Rev.* **2007**, 2, 93.
3. Deloach, L. D.; Page, R. H.; Wilke, G. D.; Payne, S. A.; Krupke, W. F. *IEEE J. Quantum Electron.* **1996**, 32, 885.
4. Page, R. H.; Schaffers, K. I.; Deloach, L. D.; Wilke, G. D.; Patel, F. D.; Tassano, J. B.; Payne, S. A.; Krupke, W. F.; Chen, T.; Burger, A. *IEEE J. Quantum Electron.* **1997**, 332, 609.
5. Sorokin, E.; Sorokina, I. T.; Page, R. H. in: OSA Trends in Optics and Photonics, Advances in Solid State Lasers Vol. 46, edited by S. Payne and C. Marshall (Optical Society of America, Washington DC, 2001), pp. 101–105.
6. Klein, P. B.; Furneaux, J. E.; Henry, R. L. *Appl. Phys. Lett.* **1983**, 42, 638.
7. Adams, J. J.; Bibeau, C.; Page, R. H.; Krol, D. M.; Furu, L. H.; Payne, S. A. *Opt. Lett.* **1998**, 24, 1720.
8. Slack, G. L.; O'Meara, B. M. *Phys. Rev.* **1967**, 163, 163.
9. Moskalev, I. S.; Fedorov, V. V.; Mirov, S. B. *Opt. Express* **2008**, 16, 4145.
10. Moskalev, I. S.; Fedorov, V. V.; Mirov, S. B.; Berry, P. A.; Schepler, K. L. ASSP Technical Digest on CD, WB30 (Opt. Soc of Am, Washington, DC, 2009).
11. Hommerich, U.; Seo, J. T.; Bluiett, A.; Turner, M.; Temple, D.; Trivedi, S. B.; Zong, H.; Kutcher, S. W.; Wang, C. C.; Chen, R. J.; Schumm, B. *J. Lumin.* **2000**, 87, 1143.
12. Trivedi, S. B.; Kutcher, S. W.; Wang, C. C.; Jagannathan, G. V.; Hommerich, U.; Bluiett, A.; Turner, M.; Seo, J. T.; Schepler, K. L.; Schumm, B.; Boyd, P. R.; Green, G. *J. Electron. Mater.* **2001**, 30, 728.
13. Bluiett, A. G.; Hommerich, U.; Shah, R. T.; Trivedi, S. B.; Kutcher, S. W.; Wang, C. C. *J. Electron. Mater.* **2002**, 31, 806.
14. Seo, J. T.; Hommerich, U.; Trivedi, S. B.; Chen, R. J.; Kutcher, S. *Opt. Commun.* **1998**, 153, 267.
15. Fedorov, V. V.; Mallory, W.; Mirov, S. B.; Hommerich, U.; Trivedi, S. B.; Palosz, W. *J. Crys. Growth* **2008**, 310, 4438.

16. Kernal, J.; Fedorov, V. V.; Gallian, A.; Mirov, S. B.; Badikov, V. V. *Opt. Express* **2005**, 1310608.
17. Fedorov, V. V.; Mirov, S. B.; Gallian, A.; Badikov, D. V.; Frolov, M. P.; Korostelin, Yu. V.; Kozlovsky, V. I.; Landman, A. I.; Podmar'kov, Yu. P.; Akimov, V. A.; Voronov, A. A. *IEEE, J. Quantum. Electron.* **2006**, 42, 907.
18. Trivedi, S. B.; Wang, C. C.; Kutcher, S.; Hommerich, Uwe; Palosz, W. *J. Cryst. Growth* **2008**, 310, 1099.
19. Aull, B.; Jenssen, H. *IEEE J. Quantum Electron.* **1982**, 18, 925.

List of Symbols, Abbreviations, and Acronyms

CdMnTe or CMT	cadmium magnesium telluride
CdS	cadmium sulfide
CdSe	cadmium selenide
CdTe	cadmium telluride
CdZnTe	cadmium zinc telluride
Co ²⁺	divalent cobalt ion
Cr ²⁺	divalent chromium ion
CVD	chemical vapor deposition
CW	continuous wave
Fe ²⁺	divalent iron ion
IED	improvised explosive device
InSb	indium antimonide
IR	infrared
IRCM	IR countermeasures
LNT	liquid nitrogen temperature
Mg	magnesium
MnTe	magnesium telluride
OPO	optical parametric oscillator
PVD	physical vapor deposition
RT	room temperature
Ti	titanium
TM	transitional metal
YAG	yttrium aluminum garnet
YLF	yttrium lithium fluoride

ZnS	zinc sulfide
ZnSe	zinc selenide
ZnSSe	zinc sulfur selenide
ZnTe	zinc telluride

NO. OF COPIES	ORGANIZATION
1	ADMNSTR DEFNS TECHL INFO CTR ATTN DTIC OCP 8725 JOHN J KINGMAN RD STE 0944 FT BELVOIR VA 22060-6218
20	US ARMY RSRCH LAB ATTN IMNE ALC HRR MAIL & RECORDS MGMT ATTN RDRL CIO LL TECHL LIB ATTN RDRL CIO MT TECHL PUB ATTN RDRL SEE M G NEWBURG J MCELHENNY J ZHANG L MERKLE M DUBINSKIY (4 COPIES) A MICHAEL N TER-GABRIELIAN T SANAMYAN (6 COPIES) V FROMZEL ADELPHI MD 20783-1197
3	BRIMROSE CORPORATION ATTN S TRIVEDI (3 COPIES) 19 LOVETON CIRCLE SPARKS MD 21152
TOTAL:	24 (1 ELEC, 23 HCs)

INTENTIONALLY LEFT BLANK.